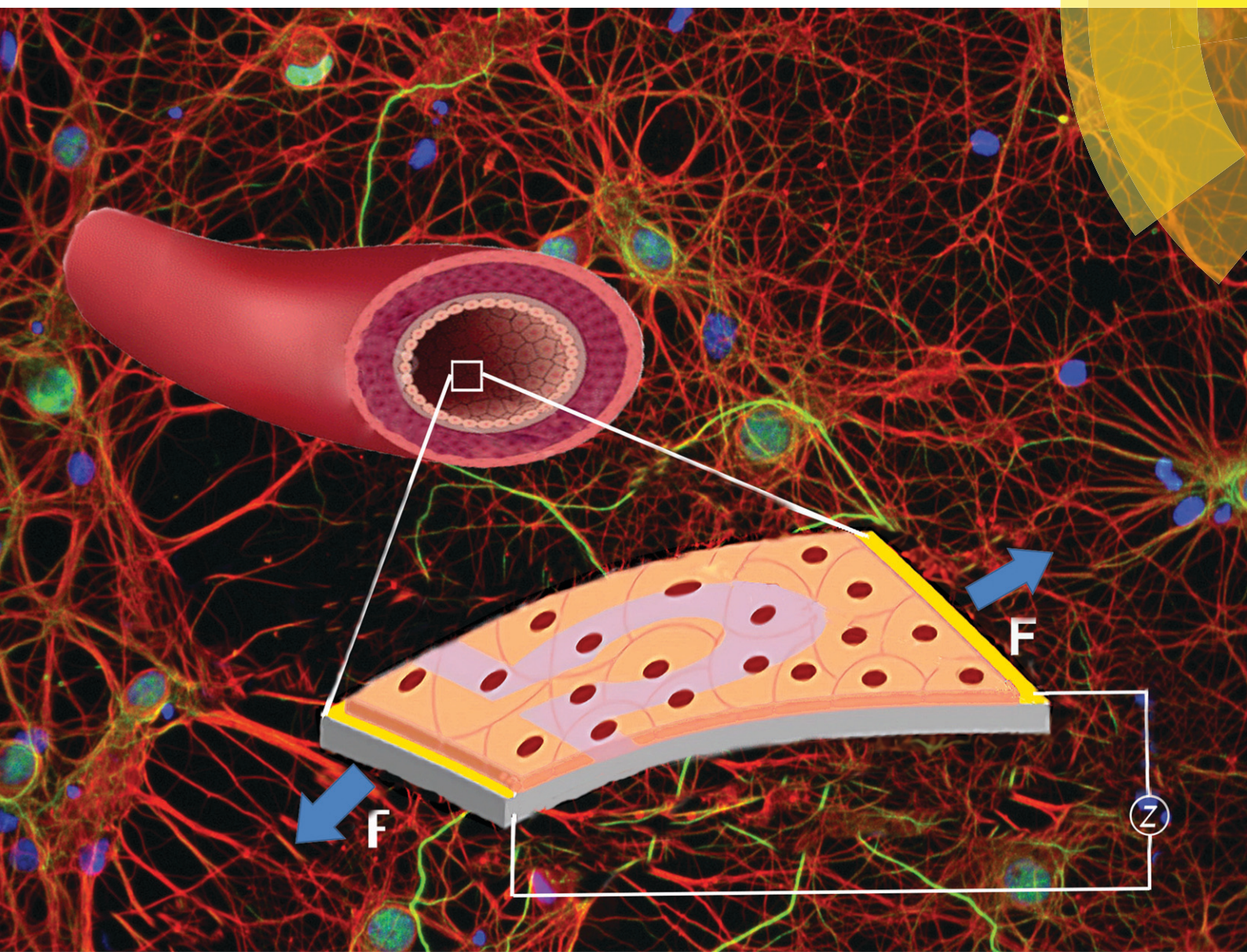


Lab on a Chip

Devices and applications at the micro- and nanoscale

rsc.li/loc



ISSN 1473-0197



ROYAL SOCIETY
OF CHEMISTRY

PAPER

Fang Li, Ioana Voiculescu *et al.*

Stretchable impedance sensor for mammalian cell proliferation measurements



Cite this: *Lab Chip*, 2017, **17**, 2054–2066

Stretchable impedance sensor for mammalian cell proliferation measurements

Xudong Zhang,^a William Wang,^{†,b} Fang Li^{*c} and Ioana Voiculescu^{*a}

This paper presents the fabrication and testing of a novel stretchable electric cell-substrate impedance sensing (ECIS) lab on a chip device. This is the first time that ECIS electrodes were fabricated on a stretchable polydimethylsiloxane (PDMS) substrate and ECIS measurements were performed on mammalian cells exposed to cyclic strain. The stretchable ECIS biosensors simulate *in vitro* the dynamic environment of organisms, such as pulsation, bending and stretching, which enables investigations on cell behavior that undergoes mechanical stimuli in biological tissue. Usually cell-based assays used in cell mechanobiology rely on endpoint cell tests, which provide a limited view on dynamic cellular mechanisms. The ECIS technique is a label-free, real-time and noninvasive method to monitor the cellular response to mechanical stimuli. Bovine aortic endothelial cells (BAECs) have been used in this research because the BAECs are exposed *in vivo* to cyclic physiologic elongation produced by blood circulation in the arteries. These innovative stretchable ECIS biosensors were used to analyze the proliferation of BAECs under different cyclic mechanical stimulations. The results of fluorescence based cell proliferation assays confirmed that the stretchable ECIS sensors were able to analyze in real-time the BAEC proliferation. The novel stretchable ECIS sensor has the ability to analyse cell proliferation, determine the cell number and density, and apply mechanical stimulation at the same time.

Received 7th April 2017,
Accepted 21st April 2017

DOI: 10.1039/c7lc00375g

rsc.li/loc

Introduction

It has been well recognized that external mechanical stimuli play important roles in regulating cellular physiological functions, such as proliferation, differentiation, morphology, and gene expression.^{1–3} Cells sense mechanical stimuli and convert them into biochemical signals through a process called “mechanotransduction”.⁴ Abnormal mechanotransduction contributes to pathophysiological process development, such as cancer metastasis and atherosclerosis.⁵ Understanding how cells actually respond to mechanical forces and how they are able to transduce these biophysical forces into biomolecular events for adaptation is vital to addressing fundamental questions about cell behaviour in both normal and pathological states.⁴

Several tools have been developed to study cell response under dynamic mechanical loadings, including atomic force microscopy,^{6,7} magnetic twisting cytometry,⁸ optical tweezers,⁹ micropipette aspiration,¹⁰ shear-flow,¹¹ and cell stretching.^{4,12–14} Cell stretching uses a deformable membrane

on which cells are cultured and stretched through the deformation of this membrane.¹⁴ This non-invasive method is capable of stimulating a large group of cells with well-controlled magnitude and direction. The cell responses are usually evaluated by standard endpoint biological assays, which are invasive and can only be carried out at endpoints. Thus, they provide a limited view on dynamic cellular mechanism. An *in situ* live-cell imaging method has been integrated into cell stretching devices to study cell responses under mechanical stretching.¹⁵ However, it requires expensive microscopy and has low throughput. During the past eight years, innovative organ-on-a-chip systems have been developed.^{16–20} These microengineered systems mimic the physiological environment of tissues *in vivo*, including complex organ-specific mechanical and biochemical microenvironments. In some organs, such as the lungs, *in vivo* mechanical stretch is critical. To replicate the lung functions *in vitro*, the lung-on-a-chip system is integrated with a biologically inspired mechanical actuation system that uses negative pressure to cyclically stretch the alveolar-capillary barrier to mimic physiological breathing motions.^{17,19,21} Organ-on-a-chip devices can be used to test the efficacy and toxicity of drugs and chemicals and to create *in vitro* models of human disease. Thus, they potentially represent low-cost alternatives to conventional animal models for pharmaceutical, chemical and environmental applications.

^aThe City College of New York, Mechanical Engineering Department, USA.

E-mail: voicules@ccny.cuny.edu

^bAmity Regional High School, Woodbridge, CT, USA

^cNew York Institute of Technology, Mechanical Engineering Department, USA.

E-mail: fli08@nyit.edu

† Currently studies at Stanford University.

Currently, most organ-on-a-chip systems rely on fluorometric labels, which can possibly affect cellular metabolism, to assess cytotoxicity.^{22–24} In addition, these methods are usually labour intensive, employ expensive microscopy or optical systems and require technical personnel to analyse data. If micro/nano scaled sensors could be integrated into the organ-on-a-chip system, it would greatly improve the throughput of the system and reduce the cost as the system would be easily automated and scaled up to larger numbers of samples. Recently, researchers started incorporating microelectrode-based sensor devices into the organ-on-a-chip system. For example, transepithelial resistance (TEER), which is formally defined as the electrical resistance across a layer of cells, has been used to examine epithelial and endothelial barrier properties in organ-on-a-chip microsystems.²⁵ Since the TEER electrodes are not on the same plane with cells, there is no need to fabricate the sensors on a stretchable substrate. However, for some powerful cell-based sensors, cells need to be cultured on the electrode surface, which brings more challenges to integrate them into organ-on-a-chip systems where *in situ* mechanical stretching of cells is required.

Electric cell-substrate impedance sensing (ECIS) is a real-time and label-free impedance-based method to study the activities of cell growth. The ECIS technique was invented by Giaever and Keese and has been extensively studied for over two decades due to its simple structure, easy operation, and sensitivity to cell behaviors and properties.^{26–28} The impedance measurements are related to cellular attachment, growth, and proliferation. When cells are seeded onto the ECIS sensor and then attach to the electrodes, the measured impedance from the ECIS sensor increases due to the insulation property of cells and reaches equilibrium when the cells are confluent and stable. When the cells detach or lose their dielectric properties due to the influence of the environment, the measured membrane impedance will decrease. As cells grow and cover the electrodes, information about the morphology of the cells and the nature of the cell attachment can be extracted from the measured impedance.^{29–32} However, the traditional ECIS sensor was fabricated on relatively rigid substrates, such as polycarbonate, glass and wafers, which cannot be stretched. That limitation disables this powerful sensor technique to be used in cell mechanobiology studies.

In the past ten years, stretchable electronics have been widely investigated. Dr. John A. Rogers' group at the University of Illinois at Urbana-Champaign invented the stretchable electronics concept.³³ They developed several stretchable sensors for monitoring the heart such as pH sensor, temperature sensor, electrocardiogram (ECG) sensor and a microscale, inorganic light-emitting diode (ILED) stretchable sensor.³⁴ These stretchable sensors were fabricated on the same membrane and provided conformal interfaces to all points on the heart with robust and non-invasive contacts enabled by the soft elasticity of the membrane itself throughout dynamic cardiac cycles.³⁵ A non-invasive, skin-mounted sensor is another application of stretchable electronics. The metallic part of the sensor is fabricated from gold with nanometer thick-

ness that is patterned into a network of serpentine ribbons for reduced stiffness and enhanced stretchability. These stretchable sensors allow electrophysiological signal measurements with ultrathin and low modulus, skin-like sheets that conformally laminate onto the surface of the skin in a manner that is mechanically invisible to the user, much like a temporary transfer tattoo.^{36–38}

Recently, several studies have been reported on stretchable electronics integrated into cell culture systems or organ-on-a-chip systems for cell monitoring. Gaio *et al.* and Khoshfetrat Pakazad *et al.* from Delft University of Technology published papers about membranes with micro electrode arrays (MEAs) fabricated from titanium nitride (TiN) and used to record the electrical activity of human pluripotent stem cell-derived cardiomyocytes (hPSC-CMs) plated on the stretchable membrane.^{20,39} However, since the flat TiN electrode was embedded in parylene layers, it is unclear about the actual strain on the TiN electrode. Liu *et al.* from Wuhan University in China reported a study on a stretchable electrode to perform cyclic voltammetry and detect the nitric oxide produced by mammalian cells when stretched.⁴⁰ Cyclic voltammetry is an electrochemical technique which uses three electrodes and is different from ECIS. In their study, one electrode is the stretchable electrode and the two auxiliary electrodes including the Ag/AgCl are outside the system. This technique requires an electrolyte which may affect the mammalian cell integrity and cannot give information about the cell morphology. Bernardeschi *et al.* developed a stretchable electrode through the formation of wrinkles on the surface of a 90 nm thick conductive layer of poly(3,4-ethylenedioxythiophene):poly(styrene sulfonate) (PEDOT:PSS) on a pre-stretched 130 μm thick poly(dimethylsiloxane) (PDMS) substrate. The electrode was demonstrated to combine good stretchability, conductivity, biocompatibility and optical transparency. Through the measurement of impedance between the two ends of a single electrode, they demonstrate the capability of conductive substrates to measure changes in ionic transmembrane currents due to mechanical stretching.¹⁴ All of the above studies show the possibility of stretchable electronics to both mechanically stimulate cells and record the response of cells from different aspects. However, there are no papers published about stretchable ECIS sensing, which is a powerful technique to study cell morphology, migration, proliferation, and differentiation.

The device presented in this study is a sensor based on the ECIS technique, fabricated on a stretchable biocompatible polydimethylsiloxane (PDMS) substrate. The stretchable electrode was fabricated by depositing a gold film on a pre-stretched PDMS substrate. In this study, instead of using chromium (Cr), a traditional material to improve the attachment between gold (Au) and polymer-based substrate, we used silane (from BMT Biosystems, Branford, CT) as adhesion promoter of the Au electrodes. Before using silane for device fabrication, we conducted several tests to study the biocompatibility of silane. Furthermore, to enhance the cell attachment to the PDMS substrate, the PDMS was treated

with oxygen plasma and subsequently with APTES to modify the surface with the chemical group $-\text{NH}_2$. The good electrical stability of the stretchable ECIS sensor enabled monitoring the mammalian cells during cyclic stretch. In this study bovine aortic endothelial cells (BAECs) were chosen to test the stretchable device because they line the inner surface of blood vessels and naturally undergo *in vivo* fluidic stress and periodic circumferential wall stretch. The ECIS impedance signature recorded over time was successfully used to analyze the cellular growth and proliferation of BAECs under the influence of cyclic mechanical stretch.

This research is novel because this is the first time that ECIS electrodes were fabricated on a stretchable PDMS substrate and ECIS measurements were performed on mammalian cells exposed to cyclic strain of 4% and 8%. In the case of this research, in order to perform impedance measurements on the cell membrane, the stretchable gold working and counter electrodes are not protected by PDMS and are directly exposed to cell media, which is an interesting and original feature of this research. Our innovative contribution to the fabrication process is focused on the strong attachment of the gold film to the substrate realized by using uncured PDMS and silane as adhesion promoter.

Materials and methods

Experimental setup

The experimental setup is shown in Fig. 1. A linear slide system (Haydon Kerk, Waterbury, CT) (Fig. 1(a)) was used to cyclically stretch the ECIS sensor array (Fig. 1(b)). As illustrated in Fig. 1(a) the sensor array contains four ECIS sensors, with

a cell culture well fabricated on top of each ECIS sensor. The linear slide system with the stretchable ECIS sensor array mounted on it were kept in a cell culture incubator during the experiment. The pitch of the thread rod of the linear slide system was 8 mm and the travel distance was 100 mm. The slide system was actuated by a stepping motor with a minimum of 0.04 mm per step. The stepping motor was driven by a Toshiba TB6560AHQ driver with a 4W1-2-phase. The four ECIS sensors included four individual working electrodes and one common counter electrode. Multiple ECIS sensors were connected to an impedance analyzer (Agilent 4294A) with a multiplexer (MAXIM DG408) (Fig. 1(c)). During the experiment, the electrical pulses were sent from the computer controlled by the Labview program. The motor driver amplified the electric pulses to drive the stepping motor to rotate at a certain angle which resulted in the movement of the linear slide to a certain distance. At the same time, the impedance data were acquired at the end of each stretch/release cycle.

In order to decide the best frequency value for performing cell membrane impedance measurements, initially the impedance values were recorded over a large frequency range. We cultured BAEC cells on the ECIS electrodes and compared the impedance values corresponding to the cell membrane with the impedance values of simple cell media. These impedance measurements were performed from 40 Hz to 100 kHz, between the ECIS working and counter electrodes using the impedance analyzer. The measurement frequency was optimized to allow the sensors to obtain the largest difference in measured impedance between a sample with and without cells.²⁹ The optimal measurement frequency was determined

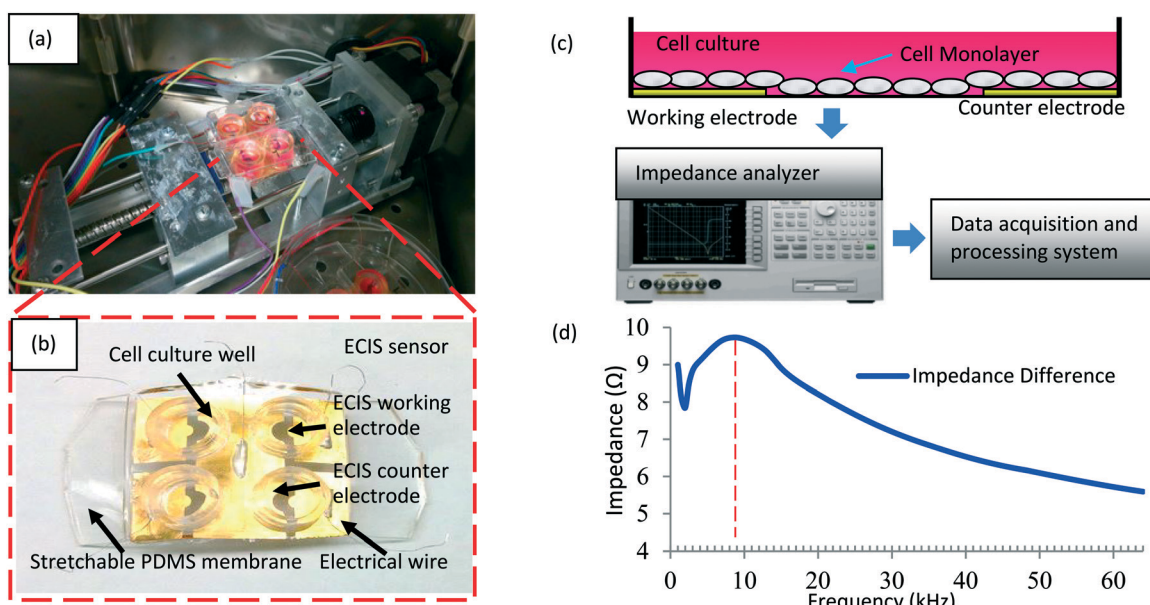


Fig. 1 (a) A linear motor was used to cyclically stretch the stretchable ECIS sensor. The linear motor with the stretchable ECIS sensor clamped on it was placed inside the incubator. (b) Stretchable ECIS sensor. (c) The stretchable ECIS sensors were connected to the impedance analyser 4294A, which applies alternating current (AC) between working and counter electrodes and acquires signal to analyse the impedance data. (d) The impedance difference between a stretchable ECIS sensor with and without cells at different frequencies.

to be 9 kHz in this study (see Fig. 1(d)). Thus, all the ECIS measurements presented in this paper were conducted with the frequency of 9 kHz.

Fabrication of stretchable ECIS sensors

The stretchable substrate of the sensor was fabricated from PDMS (Sylgard 184 silicone elastomer kit, ML SOLAR, Campbell, CA). The PDMS precursor was mixed with a crosslinking agent with a weight ratio of 10:1. The pre-polymer mixture was first kept in a desiccator to eliminate gas bubbles and later was cured at 80 °C for 4 hours. The PDMS stretchable substrate was obtained by cutting the cured PDMS polymer into rectangles of 60 mm by 44 mm. The fabrication process of the stretchable ECIS sensor is illustrated in Fig. 2(a)–(e). Initially, Au electrodes were fabricated on a glass slide and later the Au electrodes were transferred to the PDMS substrate. A gold film with a thickness of 50 nm was deposited using sputtering equipment (Hummer XP, Anatech, Union City, CA) on a clean glass slide pre-covered with a metal shadow mask (see Fig. 2(a)). The weak adhesion between gold and glass allowed the gold film to detach later from the glass slide in step (c). In this fabrication, photolithography and lift-off processes were not used to pattern the Au film because the nanometer thickness Au film fabricated on glass can be damaged during the lift-off process. (b) In order to ensure that the Au film can sustain the electrochemistry process and will not detach from the PDMS substrate, silane was used as adhesion promoter. After removal of the shadow mask, the glass slide with the patterned Au electrodes was immersed in silane (BMT Biosystems, Branford, CT) for 24 hours to improve the bonding strength of gold on PDMS. For further improvement of the Au adhesion to the PDMS substrate, besides silane, uncured PDMS was also used (see Fig. 2(c)). The glass slide with the gold electrodes covered with silane and uncured PDMS was stamped onto the pre-stretched 20% PDMS substrate. After curing the PDMS at 150

°C for 24 hours, the glass slide was peeled off from the PDMS substrate. The gold pattern adhered to the pre-stretched PDMS substrate.

An important aspect of the stretchable device is to protect the ECIS electrodes from breaking and buckling during cyclic stretching and releasing with a thin PDMS film. Openings were fabricated in the top PDMS protection film, because for performing ECIS measurements the Au film has to be in direct contact with the mammalian cells under study. The ECIS electrodes consisted of a circular working electrode and a semi-circular counter electrode. In order to obtain a thin protection film, PDMS diluted with hexane was spin-coated (2000 rpm) on the gold pattern (see Fig. 2(d)). According to the experimental results, 3.67 μm to 4.46 μm thick PDMS can be obtained if the ratio of PDMS to hexane was 1 to 100. Inductively coupled plasma (ICP) was used to etch the top protective layer of the PDMS, which was pre-covered with a shadow mask (see Fig. 2(e)). The parameters of ICP etching were electrode power of 200 W, ICP forward power of 290 W, SF₆ of 45 sccm, O₂ of 5 sccm, pressure of 7 mTorr and etching duration of 15 minutes. The shadow mask was accurately aligned on the PDMS with an alignment mold. The dimensions of the working and counter electrodes were 3.14×10^{-4} and 0.36 cm^2 , respectively, which were defined by the shadow mask. The measured electrical impedance is mainly determined by the working electrode with a very small surface area.^{41–43} The area of the counter electrode needs to be large enough to provide sufficient current paths and circuit connection. The ICP is an important fabrication step of this stretchable device because it creates openings in the top protection layer and allows the Au film of the working and counter electrodes to be exposed to the mammalian cell culture for ECIS measurements. Fig. 2(f) shows a microscopic picture of the ICP fabricated opening on the ECIS working electrode, which is circular and has a diameter of 200 μm. For culturing mammalian cells on the ECIS electrodes, circular PDMS wells were bonded on the stretchable substrate. The bonding

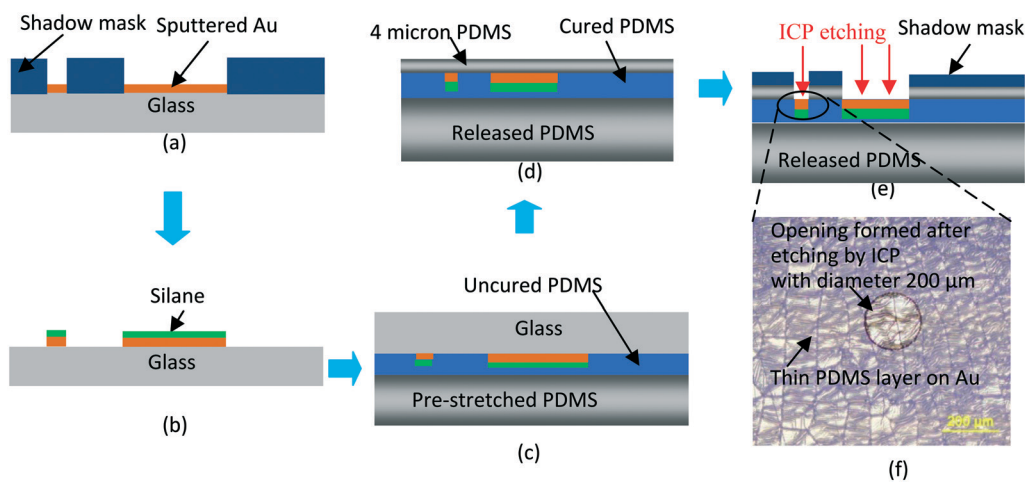


Fig. 2 (a)–(e) Schematic illustration of fabrication of stretchable ECIS sensor (not drawn to scale). (f) Microscopic image of the 200 μm circular opening in the working electrode.

consequently strengthens the mechanical property around the bonding areas. Thus, the ratio of the PDMS precursor to crosslinking, 16:1, was used in order to decrease the influence of bonding strength on the stretchable substrate. Compared with the stretchable substrate of the sensor (the ratio of PDMS precursor to crosslinking is 10:1), the cell culture wells were softer and more stretchable.

Finite element analysis of strain distribution in cell culture well

During the experiments, the stretchable substrate of the sensor was fixed at one end and stretched at the other end. The cells were seeded in the cell culture well to perform the impedance measurement. The wall of the cell culture well may additionally strengthen the stretchable substrate, which causes the decrease in the mechanical strain around the well–substrate bonding area during stretching. Thus, it was necessary to analyze the distribution of mechanical strain on the whole stretchable sensor, especially the bonding areas of the wells on the substrate.

The dimensions of the stretchable ECIS sensor were 60 mm by 44 mm by 2 mm. The thickness of the wall of the cell culture well was 1 mm. The elastic modulus of PDMS was from 1.8 MPa to 2.3 MPa with the PDMS precursor–crosslinking agent ratio of 10:1, and from 0.8 MPa to 1.0 MPa with the ratio of 16:1.^{44,45} The Poisson ratio of PDMS was from 0.45 to 0.5.^{46,47} COMSOL Multiphysics was used to analyze the distribution of strain using Hooke's law. In this simulation, the value of the Poisson ratio of PDMS was 0.499. Elastic moduli of 2 MPa and 0.9 MPa were used for the stretchable substrate of sensors and cell culture well, respectively. In order to simulate 10% mechanical stretch on the sensor, 10% mechanical strain was applied to the PDMS substrate.

Surface modification of stretchable ECIS sensor for cell attachment improvement

The surface of the stretchable sensor was covered by PDMS as a protective and insulating layer. Surface modification, including oxygen plasma treatment, chemical surface modification and ECM formation, was applied to the PDMS surface, in order to improve cell attachment on the stretchable sensor. The oxygen plasma treatment was performed using a BD-10AS High Frequency Generator (Electro-Technic Products, Chicago, IL).

For the chemical surface modification process we used (3-aminopropyl)triethoxysilane (APTES), an aminosilane usually used to modify the surface with the amine functional group ($-NH_2$). APTES (Sigma Aldrich) was diluted to 0.1% concentration using DI water. As an extracellular matrix (ECM), the sensor surface was covered with gelatin (G2500, Sigma Aldrich) diluted with Dulbecco's Phosphate-Buffered Saline (DPBS) to 0.1% concentration and fibronectin (F-1141, GIBCO, Grand Island, NY) diluted with DPBS to 30 $\mu g\ mL^{-1}$ concentration.

Cell attachment tests were performed in order to evaluate the cell attachment and biocompatibility of the original and the chemical modified PDMS. Several pieces of PDMS samples were used to simulate the PDMS substrate of sensors. Two different treatment methods were applied to PDMS samples. Cells were cultured on three groups of PDMS samples with a cell seeding density of 100 000 cells per cm^2 . The first untreated group of PDMS samples was the control group. The second group of PDMS samples was treated with oxygen plasma and 0.1% APTES. The third group of PDMS samples was treated with oxygen plasma, 0.1% APTES, 0.1% gelatin and 30 $\mu g\ mL^{-1}$ fibronectin. Cell morphology was observed under an optical microscope to confirm the formation of cell monolayers during static culture. Then cyclic stretch was performed on PDMS samples cultured with BAECs using the linear sliding system from Fig. 1(a). The cell attachment on PDMS with different types of surface modification was evaluated.

Cell culture and preparation

Bovine aortic endothelial cells (BAECs, VEC Technologies, Rensselaer, NY) were used in the experiments. The BAECs were cultured in Minimum Essential Medium (MEM, GIBCO, Grand Island, NY) with 10% fetal bovine serum (FBS, GIBCO, Grand Island NY) under standard mammalian cell culture conditions (37 °C and 5% CO₂). The stretchable ECIS sensors were coated with 0.1% gelatin (G2500, Sigma Aldrich) and kept in an incubator for 1 hour after treating with oxygen plasma for 5 minutes and 0.1% APTES for 30 minutes. Then, 30 $\mu g\ mL^{-1}$ fibronectin (F-1141, GIBCO, Grand Island, NY) was coated on the sensors and incubated for 1 hour before seeding the cells.

Cell impedance monitoring under cyclic stretch with the stretchable ECIS sensors

After surface modification was performed on the stretchable ECIS sensors, the BAECs were seeded with an initial seeding number of 30 600 cells per cm^2 . The cells firmly attached on the sensors after 24 hours of static culture on sensors. The cell impedance was measured with the ECIS technique during the experiment. All the impedance measurements were performed at the frequency of 9 kHz. After the BAECs formed a uniform monolayer the device was stretched with either 4% or 8% stretch magnitude and a cyclic stretch of 1 Hz. The cyclic stretching was performed on the BAECs for 2 or 4 hours, and the cell impedance was measured only when the sensor was in an un-stretched status. In order to investigate the effect of cyclic stretching on cell proliferation, control experiments were also performed on cell-free medium with and without cyclic stretch and on BAECs without cyclic stretching.

Cell proliferation assay

A CyQUANT Cell Proliferation Assay Kit (Life Technologies, Grand Island, NY) was used to assay the cell proliferation. The CyQUANT cell proliferation assays can measure cell

number based on measuring the DNA content. The CyQUANT reagents binding with DNA can be excited by fluorescence at 485 nm and the fluorescence emission can be detected at 530 nm. A linear equation can be obtained from the known cell numbers and detected fluorescence intensity. The linear equation can be used to assay the cell numbers according to the measured fluorescence intensity in the following experiments. The cells were extracted by trypsin (Gibco, Grand Island, NY) from each stretchable ECIS sensor at the end of the experiments and transferred to a 96-well microwell plate (Nunc, Thermo Scientific). The trypsin and medium were removed after the cell attached firmly on the substrate. Then 50 μ L CyQUANT reagent was added to each well of a 96-well microwell plate. After that, the microplate was covered and kept in an incubator at 37 °C for 30 minutes in order to allow the CyQUANT reagent to bond to the DNA. Then, the fluorescence intensity was measured with a multi-detection microplate reader (Bio-tek SynergyTM HT) to obtain the fluorescence intensity and cell number.

Results and discussion

Biocompatibility testing of silane and testing the cell attachment on PDMS with different surface modifications

Silane (custom made for this stretchable device at BMT Bio-systems, Branford, CT) was used as adhesion promoter to improve the adhesion between silicone-based polymer and gold. The cells were alive and formed a monolayer on the PDMS treated silane as shown in Fig. 3(a), which indicated that the silane has good biocompatibility.

Cell attachment on PDMS with different surface modifications was also tested in this study. The cell attachment is very weak on untreated PDMS. Most of the cells detached from the untreated PDMS after cyclic stretch as shown in Fig. 3(b). Some of the cells detached from the PDMS substrate treated with oxygen plasma and 0.1% APTES chemical modification after substrate stretch as shown in Fig. 3(c). The cells secreted ECM to provide structural and biochemical support to the surrounding cells.⁴⁸ However, the amount and concentration of secreted ECM by BAECs is not sufficient to assist cell attachment on the substrate modified by oxygen plasma and 0.1% APTES. Thus, an additional ECM pre-coating is neces-

sary to improve cell attachment on the substrate. In the third group, the cells formed a monolayer and still attached firmly on the PDMS substrate treated with oxygen plasma, 0.1% APTES chemical modification and ECM after cyclic stretch as shown in Fig. 3(d). The PDMS samples were modified with the amine group on the surface which caused the ECM to have a better adsorption profile and molecular organization for improving cell attachment. The PDMS modification process in the third group was chosen to modify the surface of stretchable ECIS sensors in this study.

Mechanical strain distribution on the sensor

Finite element analysis was used to simulate the distribution of principal strain on the device with four cell culture wells (see Fig. 4). To simulate a strain of 0.1, one end of the device was fixed and 10% mechanical stretch was applied to the opposite end. The simulated strain distribution varied from 0.096 to 0.102 on the whole area inside the cell culture wells (the colour for 0.1 strain is light blue and the whole substrate is light blue). The minimum mechanical strain of 0.096 was observed only at the bonding edge of the culture chambers and was generated by the strengthening effect of gluing the wells on the substrate. Based on this simulation we supposed that the BAECs, which formed a uniform monolayer inside the circular culture chambers and on the sensor surface, will be uniformly stretched with the same mechanical strain, because the whole area inside each culture chamber shows uniform strain. Therefore, the bond strengthening effect of cell culture wells can be neglected and the cell culture wells will stretch together with the substrate and will not hinder the uniform distribution of the mechanical strain on the BAECs. We concluded that the strain distribution on the BAECs is close to the stretching magnitude applied on the stretchable ECIS sensors.

Impedance measurement with stretchable ECIS sensors

The ECIS technique was used in this research to monitor the impedance of the BAEC membrane. In order to decide the best frequency value for performing cell membrane impedance measurements, initially the impedance values were recorded over a large frequency range. These impedance

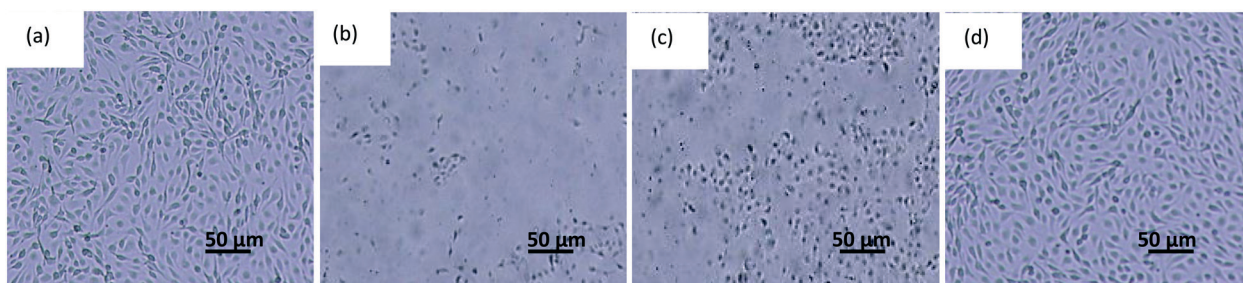


Fig. 3 Morphology of cells cultured on (a) silane treated PDMS, (b) PDMS without treatment and chemical modification after cyclic stretch, (c) PDMS treated with oxygen plasma and APTES chemical modification after cyclic stretch, (d) PDMS treated with oxygen plasma, APTES chemical modification and ECM pre-coating after cyclic stretch.

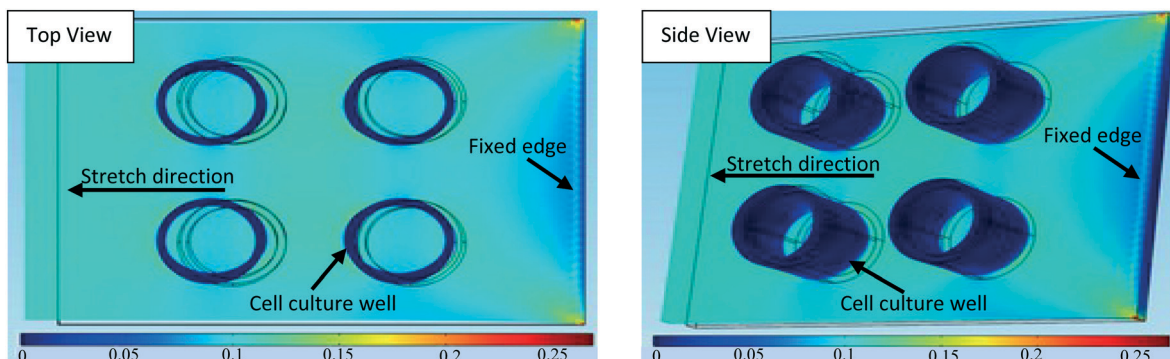


Fig. 4 Strain distribution on the stretchable sensor with four cell culture wells. The color bar indicates the mechanical strain magnitude. The sensor was fixed on the right side and stretched 10% on the left side. The black frame is the original dimension of the sensor without stretching.

measurements were performed from 40 Hz to 100 kHz, between the ECIS working and counter electrodes, using the impedance analyzer. The greatest discrepancy of impedance measurements between control wells containing only medium and wells containing cells and medium was found at 9 kHz (see Fig. 1(d)). Therefore, 9 kHz was used as the optimal frequency for all the impedance measurements presented in this paper. The normalized impedance response of cells and cell culture medium from the stretchable ECIS sensors ($n = 3$) is shown in Fig. 5(a). The normalized impedance values were obtained as the ratio between the measured cell impedance during the time of the experiment and the initial cell impedance. We repeated each experiment three times ($n = 3$). We cultured BAECs on the ECIS electrodes. The initial impedance values recorded from the culture chambers with cells were from 2707Ω to 2945Ω . The impedance of the medium was recorded with values of around 2900Ω and remained around this value for the whole time we performed the experiments. The impedance values of the cell membrane were increasing considerably in time and reached the maximum values of $14\,500 \Omega$ for stretched cells and $12\,000 \Omega$ for unstretched cells.

Fig. 5(a) shows 4% or 8% stretch with the cyclic frequency of 1 Hz applied for 2 or 4 hours. We used the frequency of 1 Hz for stretching cycles to simulate the adult heartbeat. The controls contained only cell culture medium. The solid green, pink, yellow and blue lines represent the normalized impedance of cells with stretching either from 24 hours to 26 hours or from 24 hours to 28 hours. The dashed red lines represent the normalized impedance of cells without stretching. The light green line represents the normalized impedance of cell culture medium with 8% stretching from 24 hours to 28 hours. The dashed purple lines represent the normalized impedance of cell culture medium without stretching.

In Fig. 5(a), the normalized cell impedance increased gradually after cell seeding and then reached stable values for the cells without stretching, similar to the impedance response in previous research.²⁹ All the values of normalized cell impedance did not fluctuate dramatically or shift to extremely high levels during the experiment. If the electrodes of the stretchable sensor lose their conductive ability during

the experiment, the measured impedance will shift to an extremely high level. The impedance of the controls with stretch or without stretch is overlapped in most of the areas during the cyclic stretching, which indicates that the stretchable ECIS sensors can keep a good conductive ability during cyclic stretching, because the gold electrodes were fabricated on the substrate with 20% pre-stretching. The impedance measurements were carried out when the sensors were in an un-stretched status. Even though there are cracks on the gold electrodes, 20% pre-stretching allows the electrodes to keep a good conductive ability in an un-stretched status. The impedance of the controls with or without stretching changes within 0.86% as shown in Fig. 5(a).

For the cell stretching case, the normalized impedance increased without stretching during the first 24 hours. Then the impedance decreased during 2 hours or 4 hours stretching. Based on the ECIS model introduced by Giaever and Keese with the measurement frequency of less than 40 kHz, the change in impedance is due to the changes of cell-substrate attachment and/or cell-cell contacts, which allowed the ions to travel easily between the working and the counter electrodes of the ECIS sensor.^{28–30} However, cell detachment from the substrate was not obviously observed after stretching as shown in Fig. 5(b). The normalized impedance of cells stimulated by 8% stretch is lower than that by 4% stretch as shown in Fig. 5(a). It was most likely that the stretch on cells influenced the cell–substrate attachment and/or cell-cell contacts, and higher stretch magnitude further influenced the attachment and/or junction. The stretching stopped at the time point of 26 hours or 28 hours and the normalized impedance gradually increased to the level before stretching because of the recovery of the cell–substrate attachment and cell-cell contacts. Finally, the normalized impedance of confluent cells with different stretch stimuli increased to a higher level than that without stretching as shown in Fig. 5(a). Perhaps one of the reasons was because of cell proliferation, and a higher impedance slope indicated a higher proliferation rate.^{27,49–52} Cell proliferation assays were performed to quantitatively analyze the relationship between normalized impedance and cell proliferation results at the end of the experiments.

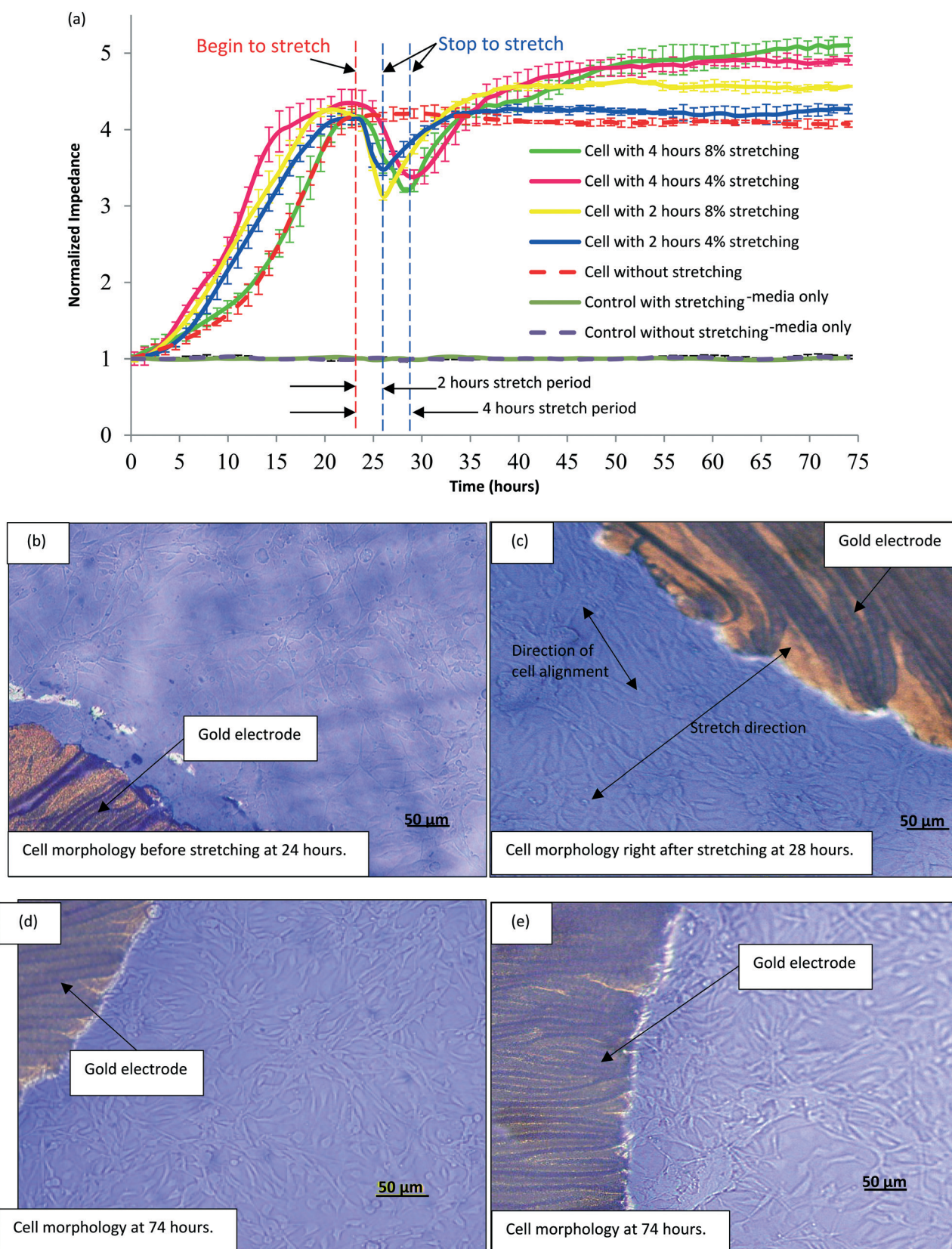


Fig. 5 (a) Normalized impedance response of cells and cell culture medium from the stretchable impedance sensors ($n = 3$). The 4% or 8% stretch with 1 Hz was only applied from 24 hours to 26 hours or from 24 hours to 28 hours. The controls contained only cell culture medium. Phase-contrast microscopy of cell morphology (b) right before stretching at 24 hours. (c) Right after (4 hours, 8% and 1 Hz) stretch stimulation at 28 hours. (d) At 74 hours (with 4 hours, 8% and 1 Hz stretch) stimulation started from 24 hours. (e) At 74 hours without stretch stimulation.

The cell morphology on the stretchable ECIS sensor right before stretching at 24 hours is shown in Fig. 5(b). The cell morphology right after 4 hours and 8% stretching at 28 hours is shown in Fig. 5(c). Some of the cells aligned perpendicular to the stretch direction. The cell morphology at the end of the experiment for cells stimulated during 4 hours with 8% stretch and cyclic frequency of 1 Hz is shown in Fig. 5(d). The cell morphology at the end of the experiment, for cells without stretch stimulation, is shown in Fig. 5(e). The focus of the microscope cannot be guaranteed to be the same everywhere for these samples because the substrate of the stretchable sensor is not exactly flat. As a result, the cell morphology in some areas is clear and in some areas is blurry.

The influence of mechanical stretch on cell proliferation

In this research we demonstrated that cell proliferation was generated by the substrate cyclic stretch and also that the real-time ECIS measurements indicate cell proliferation. Most cell-based assays rely on endpoint tests, which provide a limited view on the dynamic cellular mechanism. These endpoint analysis methods are based on optical labels and have limitations of low throughput and expensive use of cells and agents.

The ECIS measurements are performed in real time and indicate the cell states over a large period of time. Here we used BAECs because they attached to the culture well substrate. The ECIS impedance values monitor the BAECs' monolayer behaviour. When the cells are introduced in the culture wells the impedance values are low and in this study these values were between $2707\ \Omega$ and $2945\ \Omega$. After several hours in culture the cells form a uniform monolayer with higher impedance values. When the cells start to proliferate these impedance values increase.

In order to validate the information about cell proliferation obtained from the ECIS measurements, we also performed biological assays to experimentally count the number of cells. The CyQUANT Cell Proliferation Assay Kit was used to obtain the cell number. After 74 hours of experiment, as presented in Fig. 5(a) the cells were extracted from each stretchable ECIS sensor by using trypsin. In view of performing the CyQUANT cell proliferation assays the cells were transferred to a 96-well microwell plate. The CyQUANT assay is based on measurement of cellular DNA content by fluorescent dye binding. The amount of DNA in each cell remains constant for a given cell line or cell type. The cellular DNA content is closely proportional to the cell numbers. Thus, the CyQUANT cell proliferation assays based on measuring the DNA content provide an accurate measurement of cell number. The CyQUANT reagents binding with DNA were excited by fluorescence at 485 nm and emission was detected at 530 nm. A closely linear relationship was obtained from the detected fluorescence intensity and cell numbers as shown in Fig. 6(a). The linear equation can be used to assay the cell numbers according to their fluorescence intensity in

future experiments. The fluorescence intensity of cells was obtained by using the Bio-tek Synergy™ HT Multi-Detection Microplate Reader. The fluorescence intensity was transferred to the corresponding cell number according to the linear equation obtained in advance. The initial cell seeding density on the stretchable impedance sensors was 30 600 cells per cm^2 . Fig. 6(b) shows different numbers of cells corresponding to cells with different mechanical stimuli. According to Fig. 6(b), the cells stimulated by 8% stretch proliferated more than that stimulated by 4% stretch during the same stretching period (2 or 4 hours). The cells stretched for 4 hours proliferated more than cells stretched for 2 hours with the same stretching magnitude (4% or 8% stretching magnitude). The proliferation of cells without mechanical stimuli is the lowest. The ECIS records in Fig. 5(a) show that the impedance values of the stretched cells are larger than the impedance values of the un-stretched cells.

Both experimental results of different impedance values and corresponding cell numbers showed that the mechanical stretch induced the BAECs to proliferate, which is consistent with previous research.⁵² Endothelial cells lining the interior walls of blood vessels are mainly influenced by two different mechanical forces.^{54–56} Fluid shear stress is generated by the circulation of blood and the periodic stretching and relaxing of blood vessels due to blood pulsation.^{54,57–59} The production of nitric oxide (NO) by the endothelial nitric oxide synthase (eNOS) can be activated by vascular stretch.⁶⁰ NO has been proposed to be a physiological modulator of cell proliferation, cell cycle arrest, and apoptosis.⁶¹ Cyclic axial stretch in the absence of shear stress produces realignment of endothelial actin stress fibers toward the circumferential direction within a few hours.⁶² Cyclic strain can induce gene expression of monocyte chemotactic protein-1 (MCP-1) in endothelial cells.⁶³ Exposure to physiological stretch in BAECs was found to induce cell proliferation, mediated by the P13K-dependent S6 K mTOR-4E-BP1 pathway.⁵³ Mechanical stretch enables vascular maintenance through proliferation, angiogenesis, formation of reactive oxygen species, control of vascular tone and vascular remodelling.^{64–67} Mechanical stimulation on endothelial cells can activate the cells to release various substances and realign cells that might influence the cell proliferation. The experimental results showed that mechanical stimuli improved the proliferation of endothelial cells.

Here we also demonstrated that the stretchable ECIS sensors were able to determine the cell numbers. The measured impedance by ECIS was correlated to the cell number obtained by using CyQUANT cell proliferation assays. The measured cell impedance was normalized to have the same basis for comparison.

The number of cells with different mechanical stimuli after 74 hours is shown in Fig. 6(b). The corresponding impedance values for each number of cells are shown in Fig. 6(c). The relation between the cell number and the corresponding normalized impedance values is shown in Fig. 6(d). A linear correlation exists between the normalized impedance value

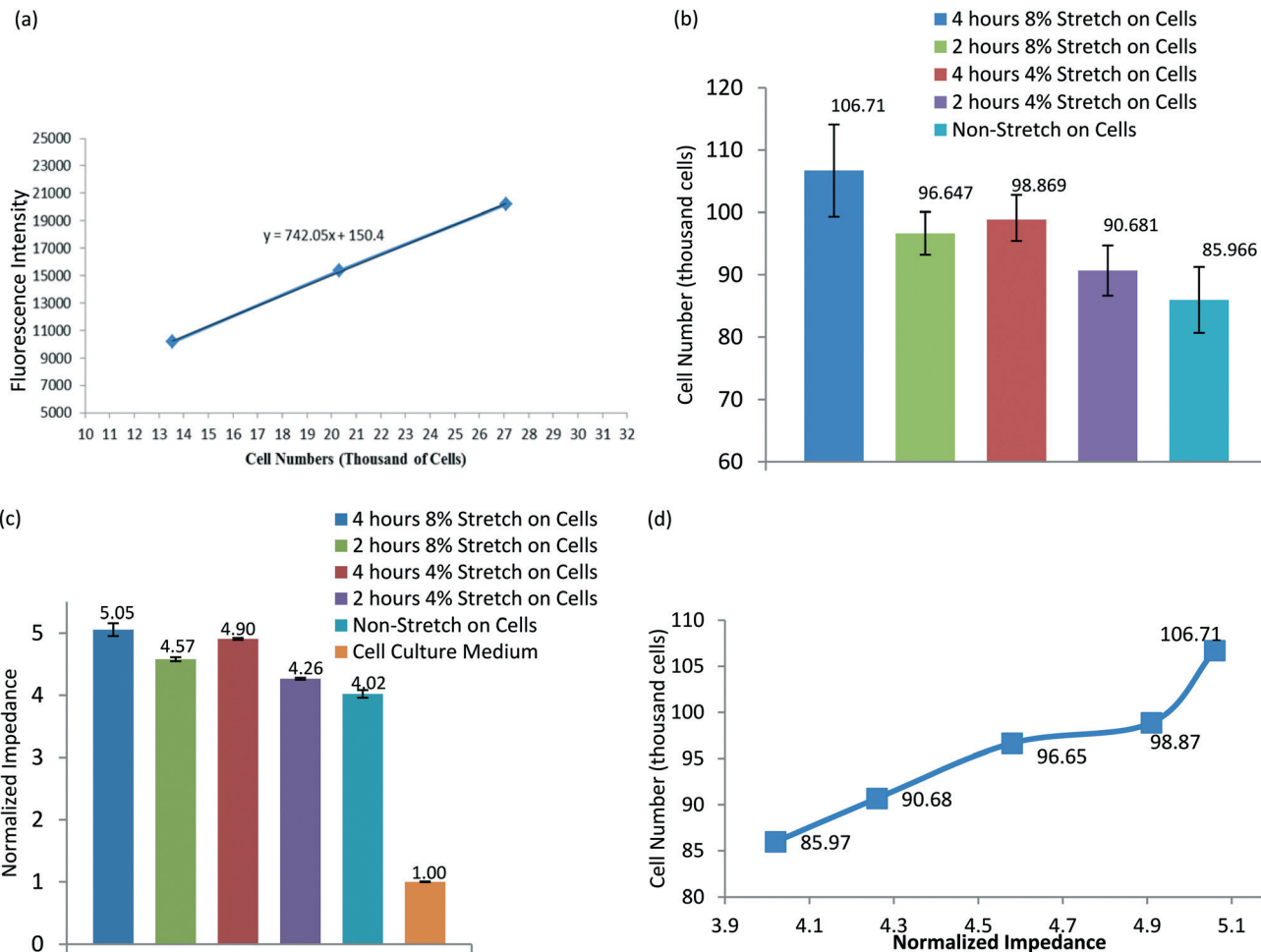


Fig. 6 (a) The relationship between cell numbers and corresponding fluorescence intensity. (b) Number of cells with different mechanical stimuli after 74 hours ($n = 3$) obtained with CyQUANT cell proliferation assays. The initial cell seeding density on the stretchable impedance sensors was 30 600 cells per cm^2 . (c) Normalized impedance values of cells with different mechanical stimuli after 74 hours ($n = 3$), corresponding to the impedance measurements from Fig. 5(a). (d) Relationship between the numbers of cells and corresponding normalized impedance.

and the cell number. Higher normalized impedance means that more cells were on the sensor. This linear correlation between normalized impedance values and cell number exists because, at the end of the experiments, the influence of stretching on the cell-substrate attachment and/or cell-cell contacts becomes insignificant and the cell density or cell number is the dominant factor that affects the impedance values. Thus, the stretchable ECIS sensors have the ability to quantitatively and non-invasively analyse the effects of mechanical stimuli on cell proliferation.

Stretching the Au film

In this research, in order to perform ECIS measurements, the stretchable gold working and counter electrodes are not protected by PDMS and are directly exposed to cell media and this is an interesting and original feature of this research. The fabrication of the stretchable and unprotected gold electrodes on the PDMS substrate was a difficult task, since the gold was exposed to cell media for a long time and

could easily exfoliate. After the gold is deposited on the pre-stretched PDMS surface, wrinkles and creaks appeared on the surface of the Au electrode after being released from the pre-stretch status (see Fig. 7(a)). A CASCADE probe station was used to evaluate the Au conductivity when cyclic stretch and release with 10% strain was applied on the substrate. The Au film resistance fluctuated between 120 Ω and 200 Ω because of cyclic stretch. The Au resistance increased when the substrate was stretched and decreased when the substrate was released, as illustrated in Fig. 7(b). Because of the variations of the Au electrode resistance the impedance data were acquired at the end of each stretch/release cycle in the non-stretched state of the device.

Initially we used only uncured PDMS to attach the Au electrodes on the cured PDMS substrate. This procedure did not give effective results. When we tested the device with BAECs after several stretching and releasing cycles the Au film was easily detached from the substrate. In order to improve the attachment of Au film on the PDMS substrate, we used silane as adhesion promoter. Before we stamped the Au

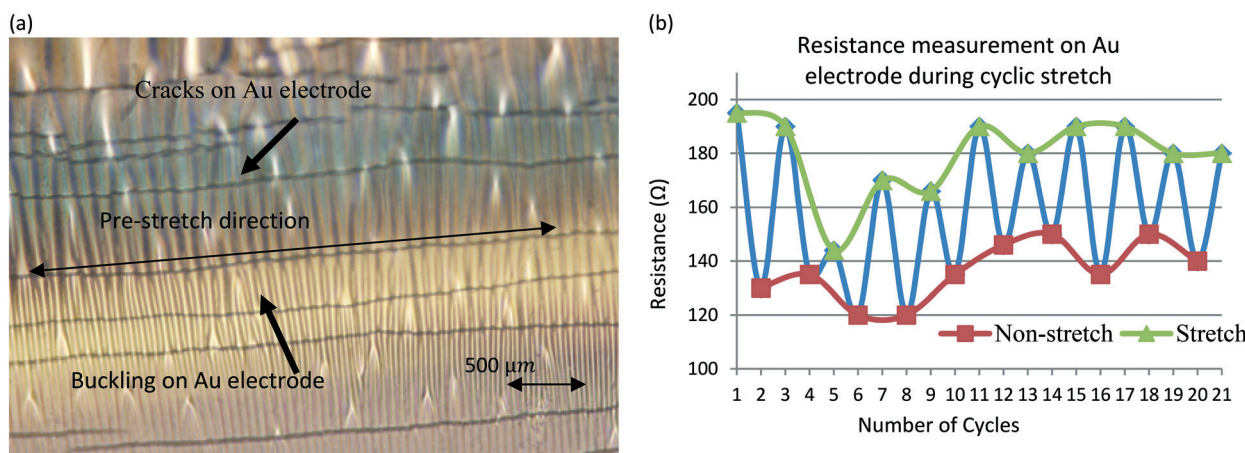


Fig. 7 (a) The profile of the Au electrode after release from 20% pre-stretch. Wrinkles and cracks appear on the surface of the Au electrode. (b) Resistance measurement on Au electrode during cyclic stretch and release with 10% strain. Resistance fluctuated between 120 Ω and 200 Ω because of cyclic stretch.

film on the PDMS surface we covered the Au film with silane. The silane improved the Au film adhesion to the PDMS substrate. We applied cyclic stretch for several hours and kept mammalian cells in culture on the Au electrodes treated with silane for several days and the Au electrode film did not detach.

As explained before, the gold film was embedded in PDMS and very small areas of the electrodes were active and in contact with cell media and cells. In order to perform the impedance measurements a small voltage of 0.9 V was applied between the working and the counter electrodes. After completing 2 hours or 4 hours of stretching and after the cell culture experiment was completed the Au electrodes were still functional.

Conclusions

In this study stretchable impedance biosensors have been developed and tested with mammalian cells. The gold ECIS electrodes were successfully fabricated on the stretchable PDMS substrate. The electrodes and electrical connection of the stretchable ECIS sensors can keep good conductivity during cyclical stretch. The elastic properties of the ECIS sensors enable the simulation and replication of the dynamic environment of organisms, in such ways as pulsation, bending and stretching. Surface modification of the hydrophobic PDMS has been carried out to optimize the sensor performance. PDMS is hydrophobic and has a low surface energy, and is not an ideal material for cell culture. In this study, the stretchable ECIS sensors with PDMS as the surface material were chemically modified to improve the cell attachment. The experimental results showed that the cells can attach firmly on stretchable ECIS sensors even during cyclical stretch. BAECs, which *in vivo* are exposed to cyclical stretch in blood vessels, have been studied. Stretchable ECIS sensors were used to analyse *in vitro* the proliferation of BAECs exposed to cyclic stretching with different

stretch magnitudes. Fluorescence based cell proliferation assays confirmed that the stretchable ECIS sensors have the ability to non-invasively and label-free analyse BAEC proliferation in real time.

In this research we demonstrated that cell stretching can influence the cell proliferation. The experiment has three steps: the first step is to culture the cells on the stretchable sensors to generate a uniform cell monolayer. The ECIS measurements showed uniform values of impedance when the monolayer is formed. The second step is to stretch the cells with the device. During the stretching process we recorded the impedance values and observed a slight diminution of the impedance values due to the enlargement of the cell-cell junction generated by the elongation. The last step is to observe the cell proliferation in the ECIS measurements after the cell stretching was stopped, and in this case we observed an increase of impedance values due to the cell proliferation. In this research we demonstrated that the novel stretchable ECIS sensors have the ability to analyse and measure the cell number, density, and proliferation and apply mechanical stimuli at the same time.

Acknowledgements

This work was supported by the US Army Research Office, grant number W911NF-10-1-0150, US Army Research Office and MIT-ISM HBCU-MI program, the US Army Centre of Environmental Health Research (USACEHR), contract number W81XWH-11-C-0026, and the Romanian National Authority for Scientific Research, CNDI-UEFISCDI project number PN-IIPT-PCCA-2011-3.2-1682. The research was also supported by a New York Institute of Technology Institutional Support for Research and Creativity (ISRC) Grant and the Professional Staff Congress/CUNY (PSC-CUNY) round 47. The content of the information does not necessarily reflect the position or the policy of the Government or MIT, and no official endorsement should be inferred.

References

- 1 D. E. Ingber, *Ann. Med.*, 2003, **35**, 564–577.
- 2 A. Buxboim, I. Ivanovska and D. Discher, *J. Cell Sci.*, 2010, **123**, 297–308.
- 3 F. H. Silver and L. M. Siperko, *Crit. Rev. Biomed. Eng.*, 2003, **31**, 255–331.
- 4 H. Kamble, M. J. Barton, M. Jun, S. Parkc and N. Nguyen, *Lab Chip*, 2016, **16**, 3193–3203.
- 5 T.-H. Kim, A. C. Rowat and E. K. Sloan, *Clin. Transl. Immunol.*, 2016, **5**, e78.
- 6 G. Thomas, N. A. Burnham, T. A. Camesano and Q. Wen, *J. Visualized Exp.*, 2013, **76**, 50497.
- 7 E. A-Hassan, W. F. Heinz, M. D. Antonik, N. P. D'Costa, S. Nageswaran, C.-A. Schoenenberger and J. H. Hoh, *Biophys. J.*, 1998, **74**, 1564–1578.
- 8 N. Wang and D. E. Ingber, *Biochem. Cell Biol.*, 1995, **73**, 327–335.
- 9 H. Zhang and K. K. Liu, *J. R. Soc., Interface*, 2008, **5**, 671–690.
- 10 L. M. Lee and A. P. Liu, *Lab Chip*, 2015, **15**, 264–273.
- 11 T. Das, T. K. Maitia and S. Chakraborty, *Lab Chip*, 2008, **8**, 1308–1318.
- 12 T. D. Brown, *J. Biomech.*, 2000, **33**, 3–14.
- 13 C. Neidlinger-Wilke, H. J. Wilke and L. Claes, *J. Orthop. Res.*, 1994, **12**, 70–78.
- 14 I. Bernardeschi, F. Greco, G. Ciofani, A. Marino, V. Mattoli, B. Mazzolai and L. Beccai, *Biomed. Microdevices*, 2015, **17**, 46.
- 15 Y. Shao, X. Tan, R. Novitski, M. Muqaddam, P. List, L. Williamson, J. Fu and A. P. Liu, *Rev. Sci. Instrum.*, 2013, **84**, 114304.
- 16 D. Huh, Y.-S. Torisawa, G. A. Hamilton, H. J. Kim and D. E. Ingber, *Lab Chip*, 2012, **12**, 2156–2164.
- 17 D. Huh, H. J. Kim, J. P. Fraser, D. E. Shea, M. Khan, A. Bahinski, G. A. Hamilton and D. E. Ingber, *Nat. Protoc.*, 2013, **8**, 2135–2157.
- 18 N. J. Douville, P. Zamankhan, Y.-C. Tung, R. Li, B. L. Vaughan, C.-F. Tai, J. White, P. J. Christensen, J. B. Grotberg and S. Takayama, *Lab Chip*, 2011, **11**, 609–619.
- 19 A. Polini, L. Prodanov, N. S. Bhise, V. Manoharan, M. R. Dokmeci and A. Khademhosseini, *Expert Opin. Drug Discovery*, 2014, **9**, 335–352.
- 20 N. Gaio, B. van Meer, W. Q. Solano, L. Bergers, A. van de Stolpe, C. Mummery, P. M. Sarro and R. Dekker, *Micromachines*, 2016, **7**, 120.
- 21 E. W. Esch, A. Bahinski and D. Huh, *Nat. Rev. Drug Discovery*, 2015, **14**, 248–260.
- 22 S. N. Bhatia and D. E. Ingber, *Nat. Biotechnol.*, 2014, **32**, 760–772.
- 23 D. Huh, *et al.* Reconstituting organ-level lung functions on a chip, *Science*, 2010, **328**, 1662–1668.
- 24 T. F. Shinawi, D. W. Kimmel and D. E. Cliffler, *Anal. Chem.*, 2013, **85**, 11677–11680.
- 25 M. Odijk, A. D. van der Meer, D. Levner, H. J. Kim, M. W. van der Helm and L. I. Segerink, *Lab Chip*, 2015, **15**, 745–752.
- 26 I. Giaever and C. R. Keese, *Proc. Natl. Acad. Sci. U. S. A.*, 1991, **88**, 7896–7900.
- 27 P. Mitra, C. R. Keese and I. Giaever, *BioTechniques*, 1991, **11**, 504–510.
- 28 C.-M. Lo, C. R. Keese and I. Giaever, *Exp. Cell Res.*, 1993, **204**, 102–109.
- 29 X. Zhang, F. Li, A. N. Nordin, J. Tarbell and I. Voiculescu, *Sens. Biosensing Res.*, 2015, **3**, 112–121.
- 30 C. R. Keese and I. Giaever, *IEEE Eng. Med. Biol. Mag.*, 1994, **13**, 402–408.
- 31 H. E. Ayliffe, A. B. Frazier and R. D. Rabbitt, *J. Microelectromech. Syst.*, 1999, **8**, 50–57.
- 32 A. Han, L. Yang and A. B. Frazier, *Clin. Cancer Res.*, 2007, **13**, 139–143.
- 33 J. A. Fan, W.-H. Yeo and J. A. Rogers, *et al.*, *Nat. Commun.*, 2014, **5**, 3266.
- 34 S. Xu, Y. Zhang and J. A. Rogers, *et al.*, *Nat. Commun.*, 2013, **4**, 1543.
- 35 L. Xu and S. R. Gutbrod, *et al.*, *Nat. Commun.*, 2014, **5**, 3329.
- 36 D.-H. Kim and J. A. Rogers, *et al.*, *Science*, 2011, **333**, 838–843.
- 37 D. Son, J. Lee and D.-H. Kim, *et al.*, *Nat. Nanotechnol.*, 2014, **9**, 397–404.
- 38 J. A. Rogers and G. Balooch, *Nat. Mater.*, 2016, **15**, 828–829.
- 39 S. K. Pakazad, A. Savov, A. van de Stolpe and R. Dekker, *J. Micromech. Microeng.*, 2014, **24**, 034003.
- 40 Y. Liu, Z. Jin, Y. Liu and X. Hu, *et al.*, *Angew. Chem., Int. Ed.*, 2016, **55**, 4537–4541.
- 41 X. Zhang, W. Wang, A. N. Nordin, F. Li and I. Voiculescu, *Sens. Actuators, B*, 2017, **247**, 780–790, in press.
- 42 X. Zhang, F. Li, A. N. Nordin, J. Tarbell and I. Voiculescu, *Sens. Biosensing Res.*, 2015, **3**, 112–121.
- 43 J. Wegener, C. R. Keese and I. Giaever, *Exp. Cell Res.*, 2000, **259**, 158–166.
- 44 Z. Qiang, Y. Zhang, J. A. Groff, K. A. Cavicchi and B. D. Vogt, *Soft Matter*, 2014, **10**, 6068–6076.
- 45 K. UweáClaussen, *RSC Adv.*, 2012, **2**, 10185–10188.
- 46 P. Du, I.-K. Lin, H. Lu and X. Zhang, *J. Micromech. Microeng.*, 2010, **20**, 095016.
- 47 V. Studer, G. Hang, A. Pandolfi, M. Ortiz, W. French Anderson and S. R. Quake, *J. Appl. Phys.*, 2004, **95**, 393–398.
- 48 G. Michel, T. Tonon, D. Scornet, J. M. Cock and B. Kloareg, *New Phytol.*, 2010, **188**, 82–97.
- 49 C.-M. Lo, C. R. Keese and I. Giaever, *Exp. Cell Res.*, 1999, **250**, 576–580.
- 50 C.-M. Lo, C. R. Keese and I. Giaever, *Biophys. J.*, 1995, **69**, 2800–2807.
- 51 R. Szulcek, H. J. Bogaard and G. P. van Nieuw Amerongen, *J. Visualized Exp.*, 2014, e51300.
- 52 C. Xiao, B. Lachance, G. Sunahara and J. H. T. Luong, *Anal. Chem.*, 2002, **74**, 1333–1339.
- 53 W. Li and B. E. Sumpio, *Am. J. Physiol. Lung Cell Mol. Physiol.*, 2005, **57**, H1591.
- 54 P. Lacolley, *Cardiovasc. Res.*, 2004, **63**, 577–579.
- 55 D. E. Berardi and J. M. Tarbell, *Cell. Mol. Bioeng.*, 2009, **2**, 320–331.

- 56 P. C. Dartsch and E. Betz, *Basic Res. Cardiol.*, 1989, **84**, 268–281.
- 57 M. Sato and T. Ohashi, *Biorheology*, 2005, **42**, 421–441.
- 58 A. Bierhaus, J. Chen, B. Liliensiek and P. P. Nawroth, *Semin. Thromb. Hemostasis*, 2000, **26**, 571–588.
- 59 J. Hatami, M. Tafazzoli-Shadpour, N. Haghhighipour, M. A. Shokrgozar and M. Janmaleki, *Exp. Mech.*, 2013, **53**, 1291–1298.
- 60 W. M. Kuebler, U. Uhlig, T. Goldmann, G. Schael, A. Kerem, K. Exner, C. Martin, E. Vollmer and S. Uhlig, *Am. J. Respir. Crit. Care Med.*, 2003, **168**, 1391–1398.
- 61 A. Villalobo, *FEBS J.*, 2006, **273**, 2329–2344.
- 62 P. Sipkema, P. J. W. van der Linden, N. Westerhof and F. C. P. Yin, *J. Biomech.*, 2003, **36**, 653–659.
- 63 B. S. Wung, J. J. Cheng, H. J. Hsieh, Y. J. Shyy and D. L. Wang, *Circ. Res.*, 1997, **81**, 1–7.
- 64 I. S. Joung, M. N. Iwamoto, Y.-T. Shiu and C. T. Quam, *Microvasc. Res.*, 2006, **71**, 1–11.
- 65 K. G. Birukov, *Antioxid. Redox Signaling*, 2009, **11**, 1651–1667.
- 66 T.-H. Cheng, N.-L. Shih, S.-Y. Chen, S.-H. Loh, P.-Y. Cheng, C.-S. Tsai, S.-H. Liu, D. L. Wang and J.-J. Chen, *J. Mol. Cell. Cardiol.*, 2001, **33**, 1805–1814.
- 67 S. Lehoux, Y. Castier and A. Tedgui, *J. Intern. Med.*, 2006, **259**, 381–392.